

Packing-induced electronic structure changes in bundled single-wall carbon nanotubes

P. Castrucci, M. Scarselli, and M. De Crescenzi

Dipartimento di Fisica, Unità INFM, Università di Roma "Tor Vergata", Via della Ricerca Scientifica 1, 00133 Roma, Italy

M. Diociaiuti and P. Chistolini

Dipartimento di Tecnologie e Salute, Istituto Superiore di Sanità, 00161 Roma, Italy

M. A. El Khakani^{a)} and F. Rosei

Institut National de la Recherche Scientifique, INRS-Énergie, Matériaux et Télécommunications 1650, Blvd. Lionel-Boulet, C.P. 1020, Varennes, Québec, Canada J3X-1S2

(Received 28 February 2005; accepted 13 July 2005; published online 30 August 2005)

The electronic structure of free-standing parallel and braided bundles of single-wall carbon nanotubes (~ 1.2 nm diameter) was probed by transmission electron microscopy and electron energy loss spectroscopy. The observed dramatic changes in the carbon $K(1s)$ near-edge structures are attributed to the tubes' structural packing in bundles which consequently alters their electronic structure. The π^* - and the σ^* -states are shown to be strongly affected by the way the tubes are packed in the bundles (i.e., parallel, braided, turned, or twisted). © 2005 American Institute of Physics. [DOI: 10.1063/1.2039989]

Single-wall carbon nanotubes (SWCNTs) are among the most widely investigated nanostructures because of their uncommon mechanical,¹ electrical,² and chemical^{3,4} properties. Their electronic behavior (metallic or semiconducting) depends on their chirality and diameter,^{5,6} twisting,⁷ bending⁸⁻¹⁰ and coiling.¹¹ Electronic properties of SWCNTs have been described theoretically in relation to the number of carbon hexagons and their matching around the tube's circumference,¹²⁻¹⁵ the distortion of the straight tubular structure,^{11,16,17} and the introduction of topological defects, such as pentagon/heptagon pairs.^{18,19} Less known are the interactions between SWCNTs within parallel²⁰⁻²⁴ and braided bundles.¹¹ In particular, the parallel packing of SWCNTs induces changes in the π^* bands formed by carbon $2p_z$ orbitals, suggesting that π bonding is the intertube binding mechanism in bundles.²⁰⁻²³ However, distortion, bending, and/or coiling individual tubes induce mixing between π and σ states.²⁵ This may change the intertube bonding character in bundles composed of distorted and/or twisted tubes, thereby locally modifying the electrical transport along the bundle and for different bundle arrangements. We recently reported a significant conductance modulation along a periodically coiled one-dimensional system made of two tightly braided nanotubes.¹¹

In this letter, we report experimental evidence for the π^* and σ^* mixed character of intertube bonding in free-standing SWCNT bundles with different packing geometries. The SWCNTs were synthesized by laser ablation, dispersed on a gold grid and examined in a transmission electron microscope (TEM) equipped with electron energy loss spectroscopy (EELS).²⁶⁻²⁸ The carbon K energy loss near-edge structure spectra of SWCNT bundles consist of the two main π^* - and σ^* -conduction bands for bulk graphite (due to strong similarities in their local atomic arrangement). We observed significant changes in the fine structure of these bands, in-

duced by structural arrangement effects, such as turning and twisting of SWCNTs into bundles.

SWCNTs were synthesized by ablating a CoNi-doped graphite target, using a pulsed Nd:YAG laser in the superposed double pulse configuration.^{29,30} TEM measurements were performed in a ZEISS 902 (80 keV) apparatus equipped with an energy filter and a Peltier cooled charge coupled device intensified PROSCAN camera.³¹ A droplet of the raw synthesis product diluted in isopropyl alcohol was used to disperse the nanotubes on a gold TEM grid (mesh 1000). Most of the reaction products are thereby located next to or bridged between two gold wires. Several TEM images identified free-standing bundles of parallel and braided nanotubes. These observations unambiguously demonstrate that small diameter nanotubes naturally self-assemble into straight or braided bundles even in the absence of an underlying substrate.

Figure 1(a) displays high-resolution TEM images of a free-standing bundle consisting of parallel-packed SWCNTs (P-SWCNT) and a free-standing SWCNT (inset), respectively. The average diameter of SWCNTs is found to be (1.2 ± 0.2) nm while that of the bundle is (22 ± 2) nm.³² Figure 1(b) shows EELS spectra recorded at the carbon K edge for: A free-standing SWCNT, a free-standing bundle of P-SWCNTs and highly oriented pyrolytic graphite (HOPG). The spectral features are due to the transition from the carbon $1s$ core level to p -like final unoccupied states.²⁶ Two prominent features are apparent: (i) The sharp peak near 286 eV, which is due to a transition from the $1s$ core level to the π^* -band, and (ii) the structures in the 293–340 eV range, due to $1s \rightarrow \sigma^*$ transitions. The former peak, attributed to the π^* -band, is characteristic of unsaturated sp^2 carbon bonds³³ and is a typical feature of the graphite K edge.^{27,33,34} However, this peak is narrower for the free-standing SWCNT (~ 1.6 eV) than for bulk graphite and the free-standing bundle of P-SWCNTs (~ 2.2 eV). This difference becomes more evident by differentiating the spectra and comparing the slope rates. The SWCNT differentiated curve [Fig. 1(c)]

^{a)} Author to whom correspondence should be addressed; electronic mail: elkhakani@emt.inrs.ca

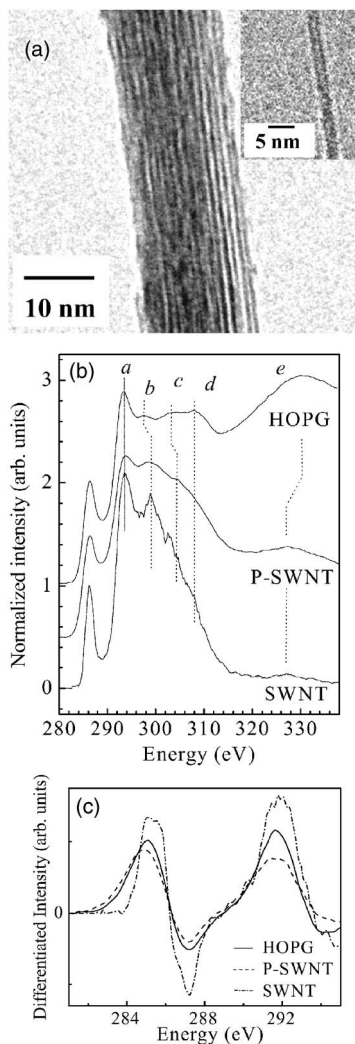


FIG. 1. (a) TEM image of a bundle of P-SWNT with a diameter of ~ 22 nm and of free-standing SWCNT with a diameter of ~ 1.2 nm (inset); (b) carbon K edge electron energy loss near edge structure of a free-standing SWCNT, a free-standing P-SWCNT bundle and a HOPG surface; and (c) enlarged part of the differentiated near-edge spectra shown in (b).

presents an onset at an energy value significantly higher than those of both other curves. This energy is strictly related to the onset of the density of unoccupied $C 2p$ states. Thus, these states are localized at energies (above the Fermi level) higher than in graphite or in P-SWCNT, implying an opening of the energy gap for the SWCNT.

Carbon K edge spectra in the 293–340 eV energy range also change, depending on the analyzed structure. The HOPG curve exhibits the typical line shape due to the $1s \rightarrow \sigma^*$ transition, composed of five prominent features (a–e). These features also appear for SWCNT and P-SWCNT samples, but present different relative intensities, widths, and energy positions with respect to HOPG. While peaks a and d do not shift, peaks b and c move toward higher energies. By contrast, peak e shows a remarkable shift toward lower energies, going from HOPG to the nanotubes. In general, the peak positions are the same for SWCNTs and bundles; however, they are much sharper for a free-standing SWCNT than for a P-SWCNT bundle. In other words, curvature affects the energy position of the σ^* -states related peaks, while tube bundling causes peak broadening. The intensity ratios of the π^* -peak to peak a (I_{π^*}/I_{σ^*}) for SWCNT and P-SWCNT

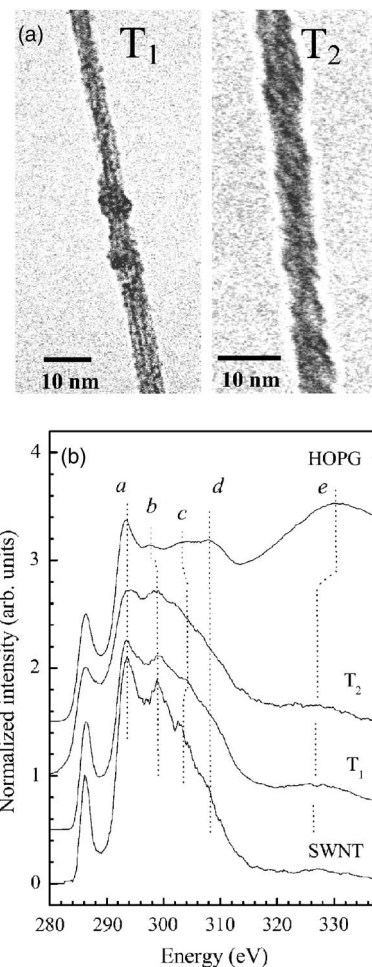


FIG. 2. (a) TEM image of two free-standing coiled SWCNT bundles with various degrees of twisting (T-SWNT); and (b) carbon K edge electron energy loss near edge structure of a free-standing SWCNT, two free-standing T-SWCNT bundles and of a HOPG specimen.

bundles (0.48 and 0.56, respectively, as opposed to 0.53 for HOPG) are in agreement with values reported by He *et al.*²³ for P-SWCNT bundles (made of ~ 1.35 nm diameter tubes) and with the tendency of the I_{π^*}/I_{σ^*} intensity ratio to increase with increasing bundle diameters. Together with the above mentioned broadening of π^* features for the P-SWCNT bundle, this confirms the already postulated π -bonding character of intertube bonding within a bundle,²³ rather than a van der Waals type of interaction (for which no changes of the energy bands are expected). Furthermore, the increase of I_{π^*}/I_{σ^*} and peak broadening can be interpreted as a result of a partial delocalization of the electrons of graphene p_z orbitals (now curved into a cylinder) and their sharing by two neighboring tubes when they approach each other. However, the simultaneous broadening of σ^* features observed in bundled tubes suggests an interaction also involving p_x and p_y orbitals, e.g., in terms of σ - π mixing.

Figure 2(a) displays TEM images of two free-standing bundles of turned and twisted SWCNTs (T-SWCNT). The average diameter of T1 and T2 bundles is (5.6 ± 0.5) nm and (6.0 ± 0.5) nm, respectively.³⁵ The corresponding carbon K edge EELS spectra are displayed in Fig. 2(b) together with those of the free-standing SWCNT and HOPG. Again, π^* and σ^* resonances change in terms of intensity ratio and width. These bundles have the same diameter, but exhibit significant differences with respect to the way they are

braided. Only a small part of the T_1 bundle undergoes turning and twisting, while the T_2 bundle is strongly coiled with an average helical angle of $(21 \pm 3)^\circ$ with respect to the tube axis. This difference in the tubes' packing geometry is reflected in the CK edge spectra [Fig. 2(b)]. Bundle T_1 does not exhibit many differences with respect to SWCNT features with a narrow π^* -peak (~ 1.8 eV) and σ^* -structure. However, its intensity ratio I_{π^*}/I_{σ^*} is ~ 0.57 , much higher than expected for a small diameter bundle of parallel tubes.²³ On the other hand, T_2 has an I_{π^*}/I_{σ^*} value of ~ 0.58 , and its π^* -peak is very broad (~ 3 eV) as are its σ^* (a-d) features, as shown by comparing the slope rates on differentiated spectra (not shown here). This demonstrates that coiling induces a strong delocalization of p_z orbital electrons, and causes strong mixing with σ^* -states. Such a rehybridization could be explained in terms of curvature-induced pyramidalization angle of carbon atoms as suggested by Niyogi *et al.*³⁶ The differentiated curve for the T_1 bundle presents an onset at an energy value which is very close to that of the SWCNT and significantly higher than that of the T_2 curve. Since this onset is related to the energy gap, we infer that the gap opening or changes in the energy gap can occur for different degrees of twisting of SWCNT bundles. In perspective, controllably coiled/braided nanotubes (with tailored energy gaps) may become fundamental building blocks for nano-electronics.

In conclusion, by combining high-resolution TEM and localized EELS measurements on free-standing laser-synthesized SWCNTs, we have shown that the packing geometry of SWCNTs in different types of bundles strongly alters their individual electronic structure.

One of the authors (M. A. E.) acknowledges financial support from NSERC of Canada and the Québec Research Network in Nanoscience (NanoQuébec). Another author (F. R.) is grateful to FQRNT (Québec) and the Canada Research Chairs program for partial salary support.

¹Carbon Nanotubes: Synthesis, Structures, and Applications, edited by M. S. Dresselhaus, G. Dresselhaus, and P. Avouris (Springer, Berlin, 2001).

²Bachtold, P. Hadley, T. Nakanishi, and C. Dekker, Science **294**, 1317 (2001).

³K. Kamaras, M. E. Itkis, H. Hu, B. Zhao, and R. C. Haddon, Science **301**, 1501 (2003).

⁴H. Oudghiri-Hassani, E. Zahidi, M. Sijaj, J. Wang, and P. H. McBreen, Appl. Surf. Sci. **212**, 4 (2003).

⁵T. W. Odom, J. L. Huang, P. Kim, and C. M. Lieber, Nature (London) **391**, 62 (1998).

⁶J. W. G. Wildöer, L. C. Venema, A. G. Rinzler, R. E. Smalley, and C. Dekker, Nature (London) **391**, 59 (1998).

⁷W. Clauss, D. J. Bergeron, and A. T. Thomson, Phys. Rev. B **58**, R4266 (1998).

⁸M. R. Falvo, G. J. Clary, R. M. Taylor II, V. Chi, F. P. Brooks Jr., S.

Washburn, and R. Superfine, Nature (London) **389**, 582 (1997).

⁹K. Suenaga, C. Colliex, and S. Ijima, Appl. Phys. Lett. **77**, 70 (2001).

¹⁰M. Ouyang, J. L. Huang, C. L. Cheung, and C. M. Lieber, Science **291**, 97 (2001).

¹¹P. Castrucci, M. Scarselli, M. De Crescenzi, M. A. El Khakani, F. Rosei, N. Braidy, and J. H. Yi, Appl. Phys. Lett. **85**, 3857 (2004).

¹²V. Meunier and P. Lambin, Phys. Rev. Lett. **81**, 5588 (1998).

¹³C. T. White and J. W. Mintmire, Nature (London) **394**, 29 (1998).

¹⁴K. Suenaga, E. Sandré, C. Colliex, C. J. Pickard, H. Kataura, and S. Ijima, Phys. Rev. B **63**, 165408 (2001).

¹⁵L. Yang and J. Han, Phys. Rev. Lett. **85**, 154 (2000).

¹⁶A. Rochefort, P. Avouris, F. Lesage, and D. R. Salhub, Phys. Rev. B **60**, 13824 (1999).

¹⁷C. L. Kane and E. J. Mele, Phys. Rev. Lett. **78**, 1932 (1997).

¹⁸S. Ihara, S. Itoh, and J. Kitakami, Phys. Rev. B **48**, 5643 (1993).

¹⁹M. Ishigami, H. J. Choi, S. Aloni, S. G. Louie, M. L. Cohen, and A. Zettl, Phys. Rev. Lett. **93**, 196803 (2004).

²⁰R. Kuzuo, M. Terauchi, M. Tanaka, and Y. Saito, Jpn. J. Appl. Phys., Part 2 **33**, L1316 (1994).

²¹M. F. Lin and D. S. Chuu, Phys. Rev. B **57**, 10183 (1998).

²²F. L. Shyu and M. F. Lin, Phys. Rev. B **60**, 14434 (1999).

²³R. R. He, H. Z. Jin, J. Zhu, Y. J. Yan, and X. H. Chen, Chem. Phys. Lett. **298**, 170 (1998).

²⁴B. W. Reed and M. Sarikaya, Phys. Rev. B **64**, 195404 (2001).

²⁵This would cause the electronic states accessible for electrical conduction to acquire a significant σ^* character.

²⁶EELS probes unoccupied electron states above the Fermi level in the energy range of core-edge levels. It yields information similar to that provided by x-ray absorption spectroscopy, assuming that the dipole transition selection rule dominates the matrix element of the scattering process.

²⁷B. M. Kincaid, A. E. Meixner, and P. M. Platzman, Phys. Rev. Lett. **40**, 1296 (1978).

²⁸TEM imaging allows to visualize and select a particular nanosystem and to study its electronic properties from a circular area with a ~ 30 nm diameter. Our measurements are not affected by any substrate interaction since we are able to select exclusively free-standing SWCNT bundles.

²⁹The target, placed in a quartz tube at the center of a furnace, was ablated with a laser intensity of $\sim 2.5 \times 10^9$ W/cm², at $T=1150$ °C in a flowing Ar gas. The synthesis product was collected on a water-cooled surface at the furnace exit. More details are reported in N. Braidy, M. A. El Khakani, and G. A. Botton, Carbon **40**, 2835 (2002).

³⁰N. Braidy, M. A. El Khakani, and G. A. Botton, Carbon **40**, 2835 (2002).

³¹The images were acquired before and after each EELS measurement to ensure that the area under investigation had not suffered any morphological change and/or damage that might result from exposure to the high-energy electron beam.

³²We obtained these values by drawing several line profiles along the tubes. All TEM images confirm that the SWCNTs have the same uniform diameter of (1.2 ± 0.2) nm, in accordance with our previous Raman results (Ref. 30).

³³G. Comelli, J. Stohr, C. J. Robinson, and W. Jark, Phys. Rev. B **38**, 7511 (1988).

³⁴R. Gunnella, I. Davoli, R. Bernardini, and M. De Crescenzi, Phys. Rev. B **52**, 17091 (1995).

³⁵The SWCNTs constituting the bundles have the same diameter (~ 1.2 nm) while the diameter of the bundles varies along a bundle and from one bundle to another.

³⁶S. Niyogi, M. A. Hamon, H. Hu, B. Zhao, P. Bhowmik, R. Sen, M. E. Itkis, and R. C. Haddon, Acc. Chem. Res. **35**, 1105 (2002).